Bull. Chem. Soc. Jpn., 72, 1351—1364 (1999)

A 12-Porphyrin System: Syntheses of Peptide Porphyrins with Multiple Histidines and the Aggregation Behavior in the Presence of Hemin

Masato Ushiyama, Atsushi Yoshino, Takeshi Yamamura,* Yasuo Shida,† and Fumio Arisaka††

Department of Chemistry, Faculty of Science, Science University of Tokyo, Kagurazaka 1-3, Shinjuku-ku, Tokyo 162-8601

†Department of Chemical Analysis, Tokyo University of Pharmacy and Life Science, 1432-1 Horinouchi, Hachioji, Tokyo 192-0392

††Department of Life Science, Faculty of Bioscience and Bioengineering, Tokyo Institute of Technology, 4259 Nagatsuta, Midori-ku, Yokohama, Kanagawa 226-8501

(Received November 30, 1998)

We succeeded in combining multiple-histidine peptides with porphyrins; that is to say, we synthesized three peptide porphyrins consisting of α_4-*meso*-tetrakis(*o*-aminophenyl)porphyrin, α_4-H_2TAPP, and amphiphilic peptide, α_4-$(PepA_{18})_n(AG)_{4-n}$-H_2TAPP (n = 1, 3, and 4; $PepA_{18}$ = EEALEKHEKALEKHEKAG), in the liquid phase. These compounds were designed to construct multiple porphyrin systems; in other words, each peptide attached on the H_2TAPP was designed to contain two histidines. The stability of the porphyrins, $(AG)_4$-H_2TAPP and $(AG)_1(Boc\text{-}AG)_3$-H_2TAPP, as well as the coupling conditions between the porphyrin fragments and the 16-residue peptide, EEALEKHEKALEKHEK, to give α_4-$(PepA_{18})_n(AG)_{4-n}$-H_2TAPP (n = 1, 3, and 4) were studied in detail with respect to the temperature, solvents, coupling reagents, additives, and amines. This search revealed that the combination of DMF/benzotriazol-1-yl-oxy-tris(pyrrolidino)phosphonium hexafluorophosphate (PyBOP)/*N*,*N*-diisopropylethylamine is suitable for the purpose. The search also clarified that it is possible to synthesize α_4-$(PepA_{18})_4$-H_2TAPP and α_4-$(PepA_{18})_3(AG)_1$-H_2TAPP selectively by choosing the coupling additives 1-hydroxy-7-azabenzotriazole (HOAt) and 1-hydroxybenzotriazole (HOBt), respectively.

All of the compounds showed 40% helicity in a solution (phospate buffer, pH = 7.0) containing 2,2,2-trifluoroethanol (TFE). The UV-vis and circular-dichroism spectrophotometric titrations of Fe(III) protoporphyrin IX chloride, **B**, with α_4-$(PepA_{18})_4$-ZnTAPP, **A**, indicated that up to three equivalents of **B** were incorporated into **A** in a buffer solution containing 15% TFE. Sedimentation-equilibrium ultracentrifugation experiments showed that **A** is a dimer in the solution, and that this dimer is transformed to a trimer when **B** is incorporated into **A**. These results suggest that **A** achieves a 12-porphyrin system consisting of different kinds of metalloporphyrin.

In the *de novo* design of artificial proteins, porphyrins occupy an important situation as effective prosthetic groups owing to their superior functionality and processibility.[1—14] In natural proteins, porphyrins (including their derivatives and chlorines) take important roles in electron transfer,[15,16] energy transfer,[17,18] and primary charge separation.[19] These functions are brought about by the integrated forms of porphyrins. For example, in the photosynthetic reaction center,[19] four chlorophylls and two pheophytins are in close contact to achieve rapid and effective primary charge separation. In light-harvesting complex[17] and the bacteriochlorophyll *a*-protein,[18] 27 and 21 chlorophylls, respectively, are also in contact with each other, or, packed in narrow molecular spaces to achieve effective energy transfer. Hemes in cytochrome c_3,[15] the photosynthetic reaction center,[19] and hydroxylamine oxidoreductase[16] are also arranged in a similar manner to achieve effective electron transfer. From this point of view, it is necessary to prepare multiple porphyrin systems in order to mimic the energy/electron transfers in nature. Although a number of artificial proteins containing porphyrins have been reported, the hexachromophore system reported by Rabanal et al. was the record of porphyrin integration.[13] The purpose of this study is to provide new

Abbreviations used are: Boc, *t*-butoxycarbonyl; CD, circular dichroism; ClZ, 2-chlorobenzyl; DIEA, *N*,*N*-diisopropylethylamine; EDC·HCl, 1-ethyl-3-(3-dimethylaminopropyl)-carbodiimide hydrochloride; ESI, electrospray ionization; HATU, *O*-(7-azabenzotriazol-1-yl)-1,1,3,3-tetramethyluronium hexafluorophosphate; HOAt, 1-hydroxy-7-azabenzotriazole; HOBt, 1-hydroxybenzotriazole; H_2TAPP, *meso*-tetrakis(*o*-aminophenyl)-porphyrin; Im, imidazole; NMM, *N*-methylmorpholine; NMP, *N*-methylpyrrolidone; OBu^t, *t*-butyl ester; OBzl, benzyl ester; OPac, phenacyl ester; PyBOP, benzotriazol-1-yl-oxy-tris-(pyrrolidino)phosphonium hexafluorophosphate; PVA, polyvinyl alcohol; TBTU, 2-(1*H*-benzotriazol-1-yl)-1,1,3,3-tetramethyluronium tetrafluoroborate; TMSOTf, trimethylsilyl trifluoromethanesulfonate; TEA, triethylamine; TFA, trifluoroacetic acid; TFE, 2,2,2-trifluoroethanol;

artificial proteins in which multiple porphyrins are in contact with each other, or packed in narrow molecular spaces.

There are three strategies for the integration of porphyrins in artificial proteins. In strategy (A), porphyrins are precedently (*a priori*) incorporated into the artificial proteins through covalent bond.[1—7] In strategy (B), porphyrins are *a posteriori* incorporated into the postulated hydrophobic area of the host proteins as guests through coordination bonds.[8—12] In strategy (C), porphyrins are incorporated into artificial proteins through covalent and coordination bonds.[13] (A) is a well-founded strategy for the incorporation of porphyrins into artificial proteins; however, the syntheses are generally complicated and the number of synthetic steps becomes large. (B) is a strategy based on solid-phase synthesis, and generally enables easy insertion of porphyrins; however, it is difficult to integrate different kinds of porphyrin. (C) is a strategy which is the most complicated, requiring a large number of steps in the liquid phase, at present. However, by using (C) it is possible to combine different kinds of porphyrin with each other; hence, increases degree of freedom in integrating porphyrins. This is advantageous for the extension of artificial proteins which are suitable in order to study electron and energy transfers.

It should be emphasized that the syntheses of multiple and hetero porphyrin systems need to bind multiple-histidine peptides to porphyrins. This causes serious problems in syntheses, because imidazole bleachs porphyrin chromophores in the presence of oxygen under illumination.[20,21] Thus, details concerning the syntheses on such systems were not yet known. In a previous communication, we reported on the synthesis of α_4-(PepA$_{18}$)$_4$-H$_2$TAPP, **9-4**, (n = 4; Fig. 1A),[22] where α_4-H$_2$TAPP = α_4-*meso*-tetrakis(*o*-aminophenyl)porphyrin[23] and PepA$_{18}$ = EEALEKHEKALEKHEKAG, according to strategy (C) based on the template-assembled synthetic proteins (TASP).[24] The zinc compound of **9-4**, α_4-(PepA$_{18}$)$_4$-ZnTAPP achieved a new record (12 porphyrins) in integrating Zn(II) and Fe(III) porphyrins.

This paper describes the experimental details concerning the syntheses of α_4-(PepA$_{18}$)$_n$(AG)$_{4-n}$-H$_2$TAPP (n = 1, **9-1**; n = 3, **9-3**; and n = 4, **9-4**). This paper also describes the aggregation of α_4-(PepA$_{18}$)$_4$-ZnTAPP, **A**, and Fe(III) protoporphyrin IX, **B**, in buffer solutions.

Figures 1B and 1C show the helical wheel and diagram of the amino acid sequence of the amphiphilic peptide PepA$_{18}$, where lysines and glutamic acids are aligned in striped forms along the postulated helical axis. This enables us to expect a two-dimensional arrangement of α_4-(PepA$_{18}$)$_4$-MTAPP (M = H$_2$ and divalent metal ions) in the solid state or in adsorbed forms on flat faces, as well as helix-bundle formation. The conformational parameters of helix and sheet (Chou–Fasman[25]) calculated for this sequence were $< P_\alpha >$ = 130 and $< P_\beta >$ = 74, respectively, and the free-energy decrease for ideal four-helix-bundle formation calculated from the solvent-accessible surface area[26] was ca. 20 kcal mol^{-1}.[27] Molecular modeling[28] by the use of computer graphics[29] and molecular-dynamics calculations on AMBER 3.1[30] showed that the distance between the two imidazole groups and that between the lower imidazole and the α_4-H$_2$TAPP were about 11 Å, whereas that from N-termini to the upper histidine were about 12 Å (Fig. 1).

Synthetic Strategy

PepA$_{18}$ was designed to include two repetitive parts made of seven residues in order to reduce the number of synthetic steps. Scheme 1 shows the synthetic route for the target compounds, **9-1**, **9-3**, and **9-4**. All of the compounds in this scheme (**1** to **8**, **9-1**, **9-3**, and **9-4**) were synthesized in the liquid phase instead of the solid phase[31,32] by the Boc strategy using phenacyl ester[33] as a C-terminal protecting group. The reason for using the liquid phase was that, from a statistical point of view, the final couplings of **6**-OH[34] to (AG)$_4$-H$_2$TAPP, **7**, and (AG)$_1$(Boc-AG)$_3$-H$_2$TAPP, **8**, require a high purity of **6**-OH.

There was a fear that direct coupling between PepA$_{18}$ and α_4-H$_2$TAPP is difficult due to a steric hindrance, as we previously pointed out.[20] Therefore, we divided the sequence of PepA$_{18}$ into two parts consisting of 16 and 2 residues, and introduced the dipeptide, Ala–Gly, to the amino groups of α_4-H$_2$TAPP to obtain **7** and **8**. This pretreatment was expected to

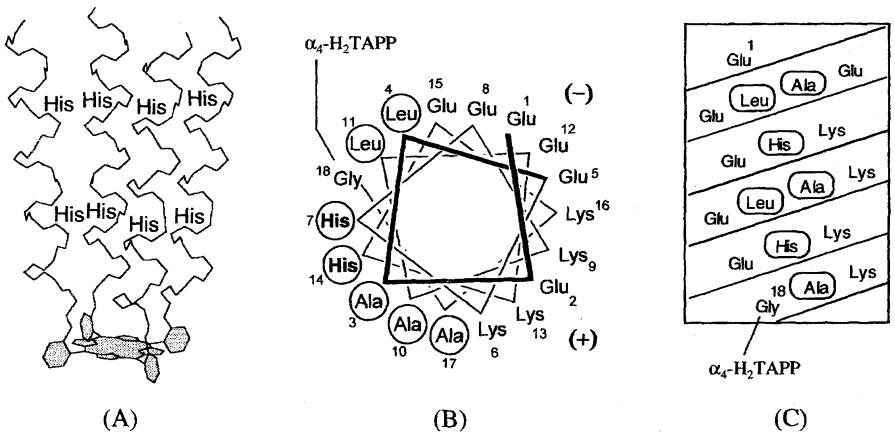

Fig. 1. (A) α_4-(PepA$_{18}$)$_4$-H$_2$TAPP. (B) Helical wheel of PepA$_{18}$. (C) Helical diagram of PepA$_{18}$.
PepA$_{18}$ = Glu–Glu–Ala–Leu–Glu–Lys–His–Glu–Lys–Ala–Leu–Glu–Lys–His–Glu–Lys–Ala–Gly.

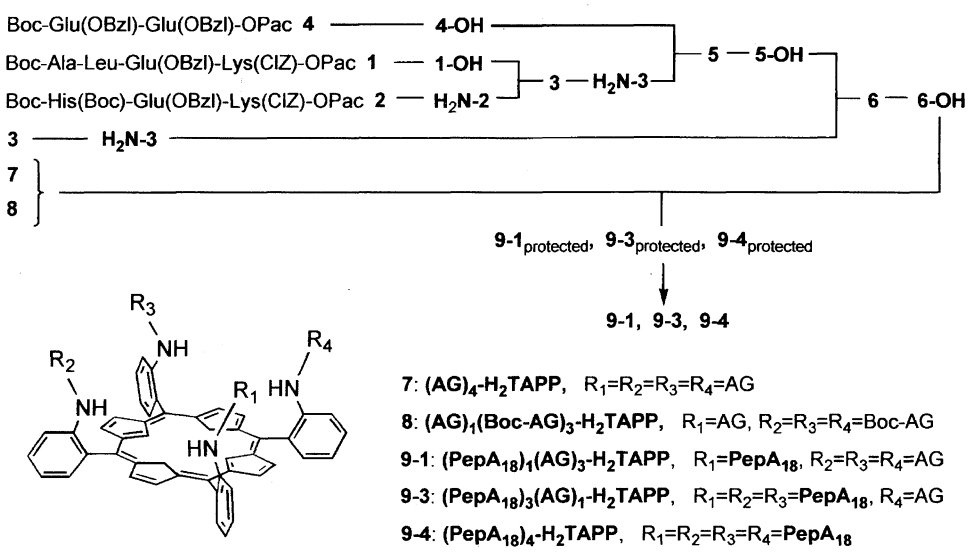

Scheme 1. Synthetic route for **9-1**, **9-3**, and **9-4**.

increase the flexibility of the reaction points of the porphyrin side, and thereby to increase the collision frequency between the peptide and porphyrin.

Because porphyrins having imidazole groups in the neighborhood are unstable, as mentioned above,[20,21] and also because our compounds have numbers of histidine, it may preferred to employ protected histidines to increase the stability of the porphyrins. However, appropriate protecting groups, which tightly protect the imidazole groups during synthesis, and can be removed efficiently at the end of the synthesis, were not found. For example, benzyloxymethyl (Bom) enables stable protection of histidine in general; however, its deprotection requires much time in some cases.[35] In addition, we observed that hydrogenolysis decomposed porphyrin chromophores probably via porphyrinogens.[36] It is generally recommended to use TMSOTf for the deprotection of Bom; however, this reaction remains 10% of uncertainty.[37,38] This value leads to approximately 57% of by-products for an 8-histidine system, such as **9-4**$_{\text{protected}}$. On the other hand, in many cases of peptide synthesis involving histidines, protection of the imidazole group is only employed at the introductory time of histidyl residue;[39] hence, unprotected histidines are actually used in peptide synthesis.[35,40—43] In consequence, in our preparation of **9-1**, **9-3**, and **9-4**, we used the protected form of His, namely Boc–His(Boc),[35] only at the starting point, in the synthesis of **2**. The imidazolyl Boc group of Boc–His(Boc) was cleaved during the next TFA deprotection step together with the N^{α}-Boc group. We made efforts to search for reaction conditions which achieved stable coupling of **7** and **8** to **6**-OH.

Results and Discussion

1. Syntheses. 1.1. Syntheses of Peptide Fragments: We observed that the synthesis of Boc–Glu(OBzl)–Lys(ClZ)–OPac is accompanied by a significant side reaction. This side reaction was efficiently suppressed according to a method of Xue et al.[44] Boc–Glu(OBzl)–Lys(ClZ)–OPac was elongated to Boc–Ala–Leu–Glu(OBzl)–Lys(ClZ)–OPac, **1**, and Boc–His(Boc)–Glu(OBzl)–Lys(ClZ)–OPac, **2**, from which Boc–Ala–Leu–Glu(OBzl)–Lys(ClZ)–His–Glu(OBzl)–Lys(ClZ)–OPac, **3**, was synthesized by the coupling.[45]

The coupling of Boc–Glu(OBzl)–Glu(OBzl)–Ala–Leu–Glu(OBzl)–Lys(ClZ)–His–Glu(OBzl)–Lys(ClZ)–OH, **5**-OH, and Ala–Leu–Glu(OBzl)–Lys(ClZ)–His–Glu(OBzl)–Lys(ClZ)–OPac, H_2N-**3**, to obtain Boc–Glu(OBzl)–Glu(OBzl)–Ala–Leu–Glu(OBzl)–Lys(ClZ)–His–Glu(OBzl)–Lys(ClZ)–Ala–Leu–Glu(OBzl)–Lys(ClZ)–His–Glu(OBzl)–Lys(ClZ)–OPac, **6**, showed the side reaction giving an isomer.[46a] In order to minimize this side reaction, various conditions were examined (Table 1).

As can be seen in Table 1, the use of HATU,[49,50] which is a well-known effective coupling reagent, not only failed to increase the yield of **6** (in DMF and DMSO), but also generated by-products other than the target compound and its isomer at room temperature. Especially, in DMSO, these side reactions became predominant, and the yield of the target compound was markedly decreased. On the other hand, the use of PyBOP in DMF achieved a sufficient yield of the target suppressing the side reaction at low temperature. Under the final conditions which we found, the reaction mixture was cooled down to −40 °C in the presence of HOBt, and gradually raised up to −25 °C for 2—3 h;[51] then, the temperature was allowed to increase to room temperature overnight.

We also observed that PyBOP caused a significant side reaction in the coupling of **3**-OH to H_2N-**3** at room temperature, which was examined as an alternative way to the method mentioned above to obtain **6** via 14-residue peptide. PyBOP generally gives sufficient results at room temperature, like BOP;[52,53] indeed, the syntheses of **3** and **5** proceeded smoothly even at room temperature. The side reactions ob-

Table 1. Reaction Conditions for the Couplings of Peptide

Entry	Condition[a)]	Solvent	*T*/°C[b)]	time/h	*Y*/%[c)]
1	**5**-OH+H_2N-**3**+PyBOP+DIEA	DMF	R.T.	2	85
2	**5**-OH+H_2N-**3**+HATU+DIEA	DMF	R.T.	1.5	41
3	**5**-OH+H_2N-**3**+HATU+DIEA	DMSO	R.T.	1	<10
4	**5**-OH+H_2N-**3**+PyBOP+DIEA	DMSO	R.T.	1	72
5	**5**-OH+H_2N-**3**+PyBOP+DIEA	DMF	−30 — R.T.	6.5	90
6	**5**-OH+H_2N-**3**+PyBOP+HOBt+DIEA	DMF	−40 — 15	20	96
7	**3**-OH+H_2N-**3**+PyBOP+DIEA[d)]	DMSO	R.T.	1	69

a) All the mixing ratios of carboxyl component/amino component/coupling reagent/amine were set at 1/1/1.2/3. b) Reaction temperature. R.T.; room temperature. Even when the reactions were carried out at R.T. DIEA was added at 0 °C. c) Yield, as analyzed by HPLC. d) The alternative route for obtaining **6**.

served in the coupling of **3**-OH and H_2N-**3**, as well as that of **5**-OH and H_2N-**3**, may be explained by the amino acid sequence of the carboxyl components, **3**-OH and **5**-OH, considering that they commonly contain His–Glu(OBzl)–Lys(ClZ)–OH.[46b–48)]

Fragment **6** was purified by preparative RP-HPLC (Asahipak ODP-50, PVA gel support) using an aqueous acetonitrile solution containing TEA as the eluent,[54)] then deprotected to **6**-OH with zinc/90% acetic acid. It is noteworthy that the post-treatment of this step should be carefully performed, because crude **6**-OH is easily contaminated with Zn^{2+}, acetic acid, and the acetate anion which bind to the histidyl imidazolate cations. The acetate group remaining on the imidazolate makes the next step; namely, the couplings of **6**-OH to **7** and **8** fall into significant failures. These contaminants of crude **6**-OH were removed by careful washing with water, ether, and an 1 M HCl aqueous solution (1 M = 1 mol dm^{-3}) several times.

1.2. Syntheses of Porphyrin Fragments: α_4-H_2TAPP was prepared according to literature methods.[23,55,56)] This was coupled to Boc–Gly with EDC·HCl in dichloromethane to give α_4-(Boc-G)$_4$-H_2TAPP, **10**. Removal of Boc from this compound and subsequent coupling of Boc–Ala gave α_4-(Boc-AG)$_4$-H_2TAPP, **11**. This was identified to be the α_4-atropisomer from a ^{1}H NMR experiment, which showed all-singlet β-pyrrole hydrogens. Generally speaking, tetraphenylporphyrins with bulky *o*-substituents are stable to atropisomerization at room temperature;[23,57)] therefore, there should be no fear of atropisomerization under the usual conditions of peptide synthesis, because they do not require heating. Finally, the controlled removal of Boc groups from **11** was performed by TFA-thioanisole to give **7** and **8**.

1.3. Condensation of the Peptide and Porphyrin Fragments:

1.3.1. Stability: In our first attempts to synthesize peptide porphyrins, the coupling of **6**-OH to **7** was done under the usual conditions (PyBOP, DMF, and room temperature) without any coupling additives. However, HPLC analyses of the reaction mixture showed many porphyrin by-products that were produced concomitantly by the decomposition of **7**. This is in contrast to the coupling of Boc–Ala to H_2N-**10**, which showed no side reactions at all. The by-products observed in the coupling of **6**-OH to **7** were attributable to destabilization of the porphyrin triggered by the imidazole groups on **6**-OH. Thus, we searched the stability of porphyrin for solvent, amine, coupling reagent, and the reaction temperature, which were prerequisite for the coupling of **6**-OH to **7**. Table 2 summarizes the result of this search. Table 2 shows that the porphyrin slightly decomposes even in DMF, itself, but is not affected by the imidazole. On the other hand, the porphyrin is remarkably unstable in DMF at room temperature in the presence of excess DIEA,[58)] which works as an initiator of the coupling reactions. The instability of porphyrin at room temperature was effectively suppressed at

Table 2. Stability of Porphyrin Fragments under Various Conditions

Entry	Condition	Mixing ratio	Solvent	*T*/°C[a)]	Result[b)]
1	**7**		DMF	R.T.	B
2	**7**		THF	R.T.	A
3	**7**+Im	1/8	DMF	R.T.	B
4	**7**+**6**-OH+DIEA	1/4/12	DMF	−15 — R.T.	B[c)]
5	**7**+PyBOP+DIEA	1/4.6/8	DMF	−15 — R.T.	C
6	**7**+DIEA	1/8	DMF	−15 — R.T.	C
7	**7**+NMM	1/8	DMF	−15 — R.T.	A
8	**7**+PyBOP	1/4.3	DMF	−15 — R.T.	A
9	**7**+TBTU	1/4.3	DMF	−15 — R.T.	C

a) R.T. means that the temperature was maintained at room temperature for over the reaction period. −15—R.T. means that the temperature was maintained at −15 °C for several hours, then allowed to stand to increase up to room temperature. b) Classified on the basis of HPLC: A, Stable for 15 h; B, Partially decomposed after 15 h; C, Decomposed within several hours. c) It was observed that **6**-OH was stable after 15 h.

low temperatures below −15 °C.

1.3.2. Coupling of 6-OH and 7 (8): Considering the results of the condition search for peptide coupling (Table 1) and porphyrin stability (Table 2), we selected PyBOP as the coupling reagent for the reaction between **6**-OH and **7** (**8**) to obtain the protected forms of α_4-(PepA$_{18}$)$_n$(AG)$_{4-n}$-H$_2$TAPP (n = 1, **9-1**$_{protected}$; n = 3, **9-3**$_{protected}$; and n = 4, **9-4**$_{protected}$). EDC·HCl was not preferable because of the formation of a considerable amount of by-products. The other coupling conditions were, then, searched for obtaining the optimum combination of the solvent, amine, reaction temperature, and coupling additive. The results are given in Table 3. The reaction efficiency was estimated from the RP-HPLC peaks of the deprotected products (those of protected compounds were not used for this estimation because of the insufficient peak detectability).

Among the solvents examined here (DMF, THF, and NMP), THF was not suitable for the reaction, because it decomposed **7** in the presence of PyBOP (see Table 1), although **7** was stable in THF without PyBOP. DMF and NMP are recognized to be similar to each other as solvents for peptide synthesis; however, considering the results of the presearch in Tables 1 and 2, DMF was selected because of its low freezing point. In practice, DMF allowed us to lower the reaction temperature sufficiently to diminish the amount of by-products in the coupling of **6**-OH to **7** and **8**. In the final procedure, the reaction temperature was set at −45 °C at the starting point, similarly to the coupling of **5**-OH to H$_2$N-**3** (Table 1), then, gradually raised up until completion of the reaction.

The use of coupling additives, HOBt and HOAt, together with PyBOP was effective in diminishing the by-products. The combination of PyBOP and HOAt gave a sufficient yield for the synthesis of **9-4**$_{protected}$, whereas that of PyBOP and HOBt caused by-products together with **9-4**$_{protected}$. However, it is noticed that the latter combination was effective to give **9-3**$_{protected}$ within several hours below −10 °C. As pointed out in the literature,[49,50] HOAt enhances the efficiency of peptide couplings in the presence of PyBOP, especially when the reactions do not complete by HOBt due to a large steric hindrance. Thus, it is possible to synthesize **9-3**$_{protected}$ and **9-4**$_{protected}$ independently by the choice of HOBt and HOAt.

It should be emphasized that the coupling reaction between **6**-OH and **8** to obtain **9-1** was very sensitive to the impurities (CH_3COOH and Zn^{2+}) included in **6**-OH. These contaminants gave such by-products as acetylated compounds, α_4-(Ac-AG)$_1$(AG)$_3$-H$_2$TAPP, and the zinc porphyrins. Furthermore, we observed an inclusion compound consisting of **8** and pyrrolidine, which originated from PyBOP in some cases.

1.3.3. Deprotections and Purifications: Final deprotections of **9-1**$_{protected}$, **9-3**$_{protected}$, and **9-4**$_{protected}$ to **9-1**, **9-3**, and **9-4**, respectively, were carried out using TMSOTf-thioanisole in TFA.[37,38] The target compounds were purified on an RP-HPLC (Fig. 2). The observed mass numbers by ESI mass spectrometry for the purified compounds agreed with theoretical ones, as shown in Fig. 3.

Compound **9-1** was easily purified by HPLC, whereas the separation of **9-3** and **9-4** was significantly dependent on the types of the columns applied. In the cases of **9-3** and **9-4**, the peak separations among these compounds and the by-products were insufficient, and their peak exhibited remarkable line broadenings for some columns. Thus,

Table 3. Reaction Conditions for the Coupling of Peptide Fragment **6**-OH to Porphyrin Fragment **7**

Entry	Condition	Mixing ratio	Solvent	T/°C[a]	Result[b]
1	**6**-OH+**7**+PyBOP+DIEA	8/1/10/20	DMF	0 — R.T.	b C
2	**6**-OH+**7**+PyBOP+DIEA	4/1/4.4/12	DMF	−40 — R.T.	b C
3	**6**-OH+**7**+PyBOP+DIEA	4/1/4.3/12	DMF	−40 — −5	b B[c]
4	**6**-OH+**7**+PyBOP+DIEA	4/1/4.3/12	THF	−40 — 15	b —
5	**6**-OH+**7**+PyBOP+NMM	4/1/4.3/12	DMF	−40 — 15	b B[c]
6	**6**-OH+**7**+PyBOP+DIEA	4/1/4.3/12	DMF	−15 — 15	b —
7	**6**-OH+**7**+PyBOP+DIEA	4/1/4.3/12	NMP	−15 — 15	b —
8	**6**-OH+PyBOP+DIEA	1/1.1/2	NMP	−15 — 15	c –
9	**6**-OH+EDC·HCl+HOBt	1/1.1/1.1	NMP	−15 — 15	c —
10	**6**-OH+**7**+PyBOP+HOBt+DIEA	4/1/4.3/4.3/12	DMF	−45 — −10	a B
11	**6**-OH+**7**+PyBOP+HOBt+DIEA	4/1/5/6/12	DMF	−15 — 40	b A[c]
12	**6**-OH+**7**+PyBOP+HOBt+DIEA	6/1/8.3/9/16	DMF	−45 — R.T.	a A[c]
13	**6**-OH+**7**+PyBOP+HOBt+DIEA	3/1/4/4.5/10	DMF	−45 — −8	a B
14	**6**-OH+**7**+PyBOP+HOAt+DIEA	6/1/8.3/9/16	DMF	−45 — R.T.	a A
15	**6**-OH+**7**+PyBOP+HOAt+DIEA	4/1/5/6/12	DMF	−45 — R.T.	a B

a) Reaction temperature: 0—R.T. means that the temperature was maintained at 0 °C for several hours, then allowed to stand to increase up to room temperature. b) Classifications of the results on the basis of HPLC. The left column shows the results on the coupling reaction: a, Major products gave the target compounds, **9-3**$_{protected}$ and **9-4**$_{protected}$ although small amounts of by-products were observed in HPLC; b, Increased amount of by-products were observed comparing with the cases a; c, Partially decomposed after several hours. The right column shows those on the deprotection reaction: A, **9-4** was mainly formed; B, **9-3** was mainly formed; C, Many by-products were formed. c) Many by-products were observed and the yield of the target compound was low.

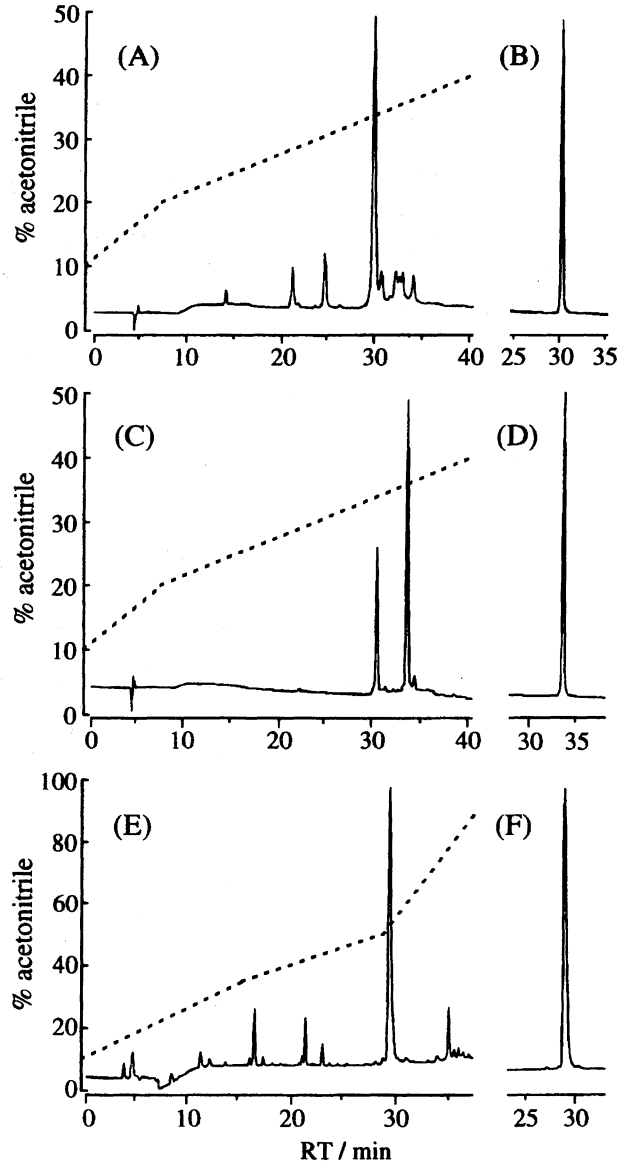

Fig. 2. Analytical RP-HPLC of (A) crude **9-4**, (B) purified **9-4**, (C) crude **9-3**, (D) purified **9-3**, (E) crude **9-1**, and (F) purified **9-1**. Chromatography was performed using a gradient of aqueous acetonitrile containing 0.05% TFA (acetonitrile concentration is represented by dotted line); 0.8 ml min^{-1}; 210 nm detection.

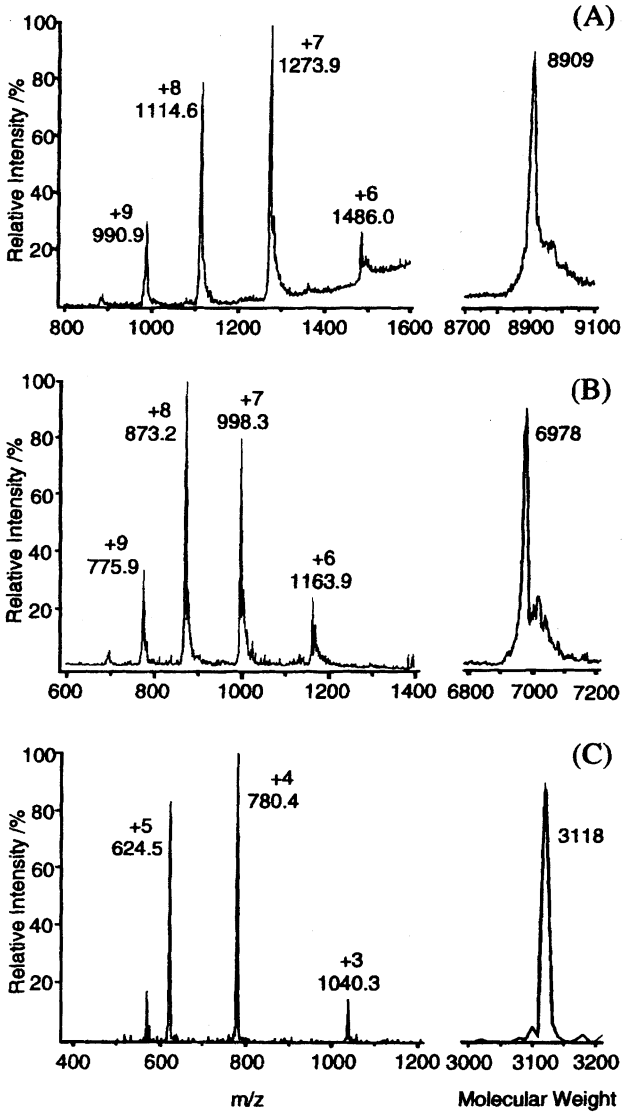

Fig. 3. ESI mass spectra: (A) α_4-($PepA_{18}$)$_4$-H_2TAPP, **9-4** (M_{calcd} = 8908); (B) α_4-($PepA_{18}$)$_3$(AG)$_1$-H_2TAPP, **9-3** (M_{calcd} = 6978); (C) α_4-($PepA_{18}$)$_1$(AG)$_3$-H_2TAPP, **9-1** (M_{calcd} = 3118). Left side: multiple-charge state. Right side: reconstructed single-charge state.

eight commercially available columns were inspected with respect to alkyl chain length (C_{18} and C_4), micropore sizes (100 and 300 Å), supports (silica and PVA), and mobile phases (TFA and phosphate). Although the relationship between these properties and the separation ability was not clear, used Shim-pack CLC-ODS(M) (Shimadzu) and Shim-pack PREP-ODS(H) (Shimadzu) and newly purchased CAPCELLPAK C_{18} SG300 (Shiseido) gave satisfactory results. Considering that CAPCELLPAK C_{18} SG300 adopts highly pure silica gel with very low metal contents as its support, the column dependence mentioned above may be explained by the interaction between the coordinative residues in $PepA_{18}$, such as glutamic acid and histidine, and by metal impurities in the support.[59,60] However, CAPCELLPAK C_{18} UG120 (Shiseido), which adopts a highly pure silica gel, showed broad peaks. UG120 is different from SG300 in the pore sizes (120 Å for UG120 and 300 Å for SG300), suggesting that the micropore size also affects the separability.

2. Aggregation Properties. The hexaporphyrin system reported by Rabanal et al.[13] (designed as a maquette of the photosynthetic reaction center) was constructed in a four-helix bundle by incorporating two Fe protoporphyrin IX, hemin, as the prosthetic groups. The bundle is composed of dimeric artificial proteins, each of which contains coproporphyrin and a disulfide-bridged two-helix peptide. Robertson et al. reported a tetraporphyrin system, which contains four Fe protoporphyrins as prosthetic groups,[11] intending for a metalloprotein maquette. Rau et al. reported a diporphyrin system in order to model Cytochrome b,[8] and Mihara et al.

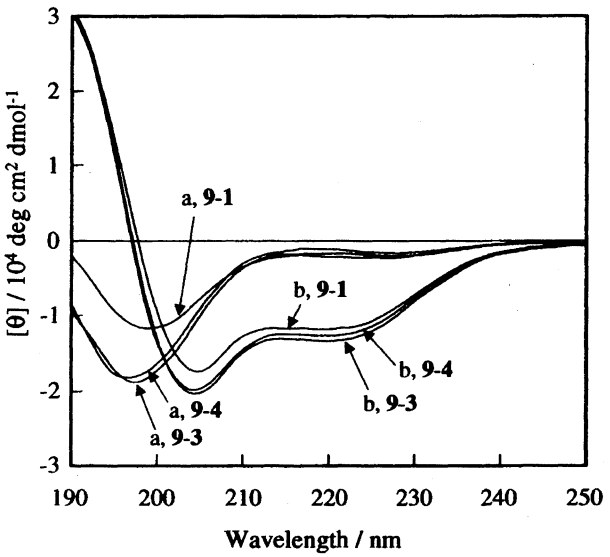

Fig. 4. CD spectra of target compounds **9-1** ($c = 3\times10^{-5}$ M), **9-3** ($c = 1\times10^{-5}$ M), and **9-4** ($c = 1\times10^{-5}$ M). Solvent: a, 25 mM phosphate buffer pH 7.0; b, 25 mM phosphate buffer pH 7.0 containing 40% TFE.

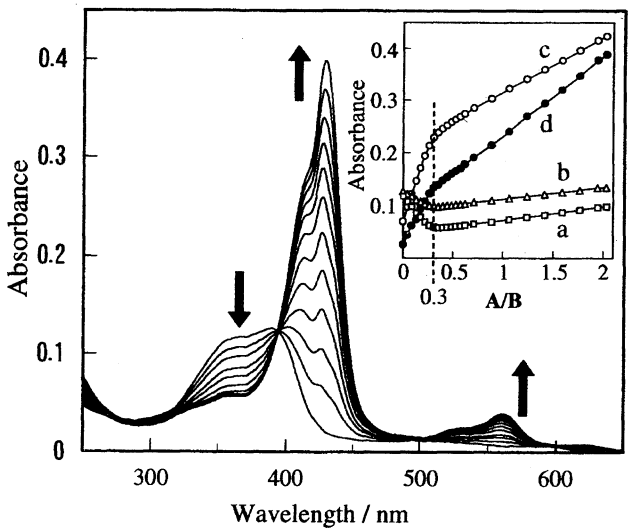

Fig. 5. UV-vis spectral changes. 21 μM of **B** was titrated by 75 μM of **A** at **A/B** ratios = 0.0, 0.04, 0.09, 0.13, 0.18, 0.22, 0.27, 0.31, 0.35, 0.40, 0.44, 0.49, 0.53, 0.57, 0.62, 0.71, 0.88, 1.1, 1.2, 1.4, 1.6, 1.8, 1.9, and 2.0. Spectra for **A/B** ratio = 0.53 and above are not shown here for clarity. Arrows show the trends of changes on titration. Inset: titration curves monitored at 364 (a, □), 389 (b, △), 410 (c, ○), and 560 nm (d, ●). The plots of the 560 nm are shown as the fourfold values of measured absorbances.

reported a disulfide-bridged two-helix peptide, which realized a chiral assembly of two tetraphenylporphyrin derivatives at the lysine residues.[1)]

In this study, we adopted Fe(III) protoporphyrin IX (**B**) as the prosthetic group to be incorporated into the hydrophobic multiple-histidine area of α_4-(PepA$_{18}$)$_4$-ZnTAPP (**A**). This combination is suitable for studying the aggregation properties by spectrophotometric methods, as well as of photo-induced redox reaction, because of the clear difference in λ_{max} and the line shape. Thus, UV-vis absorption and CD titrations were performed in order to clarify the number of **B** incorporated into **A** and the conformational change of peptides and porphyrins, respectively. The molecular weights of the aggregates were also studied by sedimentation-equilibrium ultracentrifugation.

2.1. CD Spectra. The CD spectra of the metal-free bases (**9-1**, **9-3**, and **9-4**) in solutions are shown in Fig. 4. In buffer solutions, they show strong negative bands below 200 nm, which indicates that the peptide moieties of these compounds are predominantly in random coil conformations. In a buffer solution containing 40% TFE, which is known to be a helix-enhancing reagent,[61)] each spectrum shows two minima near 222 and 206 nm and a maximum near 190 nm. The helicities calculated from the mean residue ellipticity at 222 nm ($[\theta]_{222}$),[62,63)] were ca. 40% for all the cases of **9-1**, **9-3**, and **9-4**. This means that the conformational behavior of **9-1**, **9-3**, and **9-4** are independent on the number of peptides on the porphyrin. This also means that there would be no increase in helicities due to helix bundle formation among the helices of **9-3** and **9-4**. The low helicity seems to be caused by multiple histidine residues, which generally destabilize the helix formation.

2.2. Incorporation of Hemin. A preliminary study on α_4-(PepA$_{18}$)$_4$-ZnTAPP, **A**, by CD spectroscopy revealed that this compound has 7—38% helicity (calculated from $[\theta]_{222}$) in the buffer solution containing 0—50% TFE similarly to those of the free bases, **9-1**, **9-3**, and **9-4**. The spectrophotometric titrations on **A/B**, described below, were performed in a solution with 15% TFE, in which **A** alone showed 16% helicity.

The titrations were performed in the manner **B** into **A** according to the literature on the reconstitution of apomyoglobin,[64)] which has been adopted for hemin titration in the field of *de novo* designed proteins.[10,12)] Considering that the pK_a value of the His imidazole group is 6.0, we conducted the incorporation at pH 7.0 using a phosphate buffer, where the theoretical charge number of **A**, calculated from the pK_as of the amino-acid residues, equals −3.

The results of the UV-vis titration of **B** with **A** are shown in Fig. 5, where **B** shows broad bands at 364 and 389 nm suggestive of aggregates formation. When **A** was successively added into the solution of **B**, the intensities of these broad peaks gradually decreased while new peaks gave rise to at 410 and 428 nm. This result suggests that the hemin molecules transfer from the aggregates to **A**. The titration curves observed at appropriate wavelength points show that their turning points lie at about **A/B** = 1/3 (Fig. 5, see inset). This indicates that up to three equivalents of **B** molecules are incorporated into **A**.

The CD spectral changes in vis and UV regions corresponding to those of absorption changes mentioned above are shown in Figs. 6A and 6B. In the Soret band region (Fig. 6A), the titration curves at appropriate wavelengths show that their turning and inflection points exist at about **A/B** = 1/3, corresponding to the absorption changes (Fig. 5,

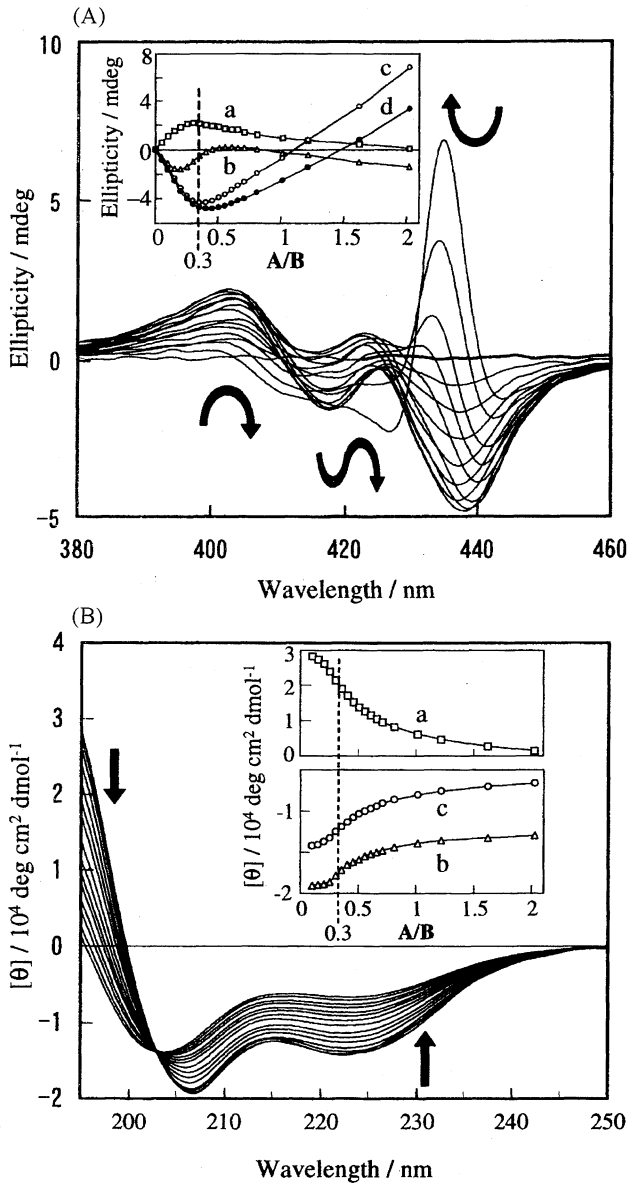

Fig. 6. CD spectral changes. 21 μM of **B** was titrated with 75 μM of **A** at **A/B** ratios = 0.0, 0.05, 0.10, 0.15, 0.20, 0.25, 0.30, 0.35, 0.40, 0.46, 0.51, 0.56, 0.61, 0.66, 0.71, 0.81, 1.0, 1.2, 1.6, and 2.0. Arrows show the trends of changes on titration. (A) Spectral changes in vis region. Spectra for **A/B** ratios = 0.35, 0.46, 0.56, 0.66, and 0.71 are not shown here for clarity. Inset: titration curves monitored at 403 (a, □), 417 (b, △), 435 (c, ○), and 438 (d, ●) nm. (B) Spectral changes in UV region. Spectra for **A/B** ratios = 0.0, 0.05, 0.46, 0.56, and 0.66 are not shown for clarity. Inset: titration curves monitored at 195 (a, □), 206 (b, △), and 222 (c, ○) nm.

inset). On the other hand, the CD spectral change in the Soret band region seems to have several isodichroic points accompanied by changes in the peak positions, linewidths, and intensities. Although it may be difficult to understand from the figures, these complicated changes in the CD spectra correspond to those in the UV-vis absorptions in Fig. 5. These changes can be attributed to those originating from exciton couplings. They suggest that **A** and **B** are located close to each other in the molecular space and change their mutual configurations when the **A/B** ratio is increased.

The CD spectral change in the UV region (Fig. 6B) shows an increase of the helicity of **A** in the presence of a sufficient amount of **B** (**A/B** ≤ 0.3). The helicity change was from 16 to 45% (calculated from $[\theta]_{222}$). Hemin promotes helix formation when it incorporates into **A**, as mentioned in other reports.[10,12] The titration curves also show inflection points at about **A/B** = 1/3. The observed low helicities are explained by the existence of His residues which are free from coordination to **B** in $PepA_{18}$. The histidyl residue is well known to generally destabilize helix formation, and **A** was designed to contain a number of His residues, thus sacrificing helicity in order to incorporate multiple porphyrins.

Sedimentation-equilibrium ultracentrifugation experiments were performed for buffer solutions containing only

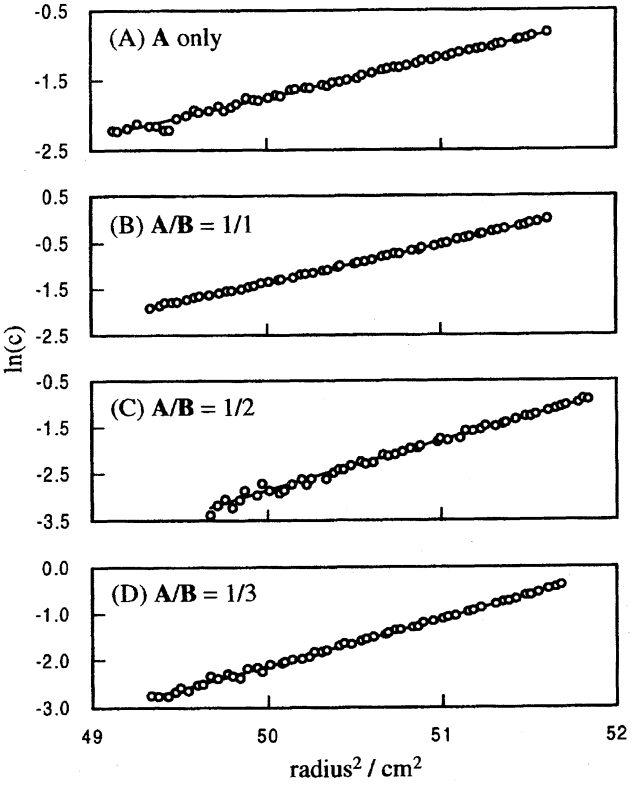

Fig. 7. Profiles of sedimentation-equilibrium ultracentrifugation of (A) **A** only, (B) **A/B** = 1/1, (C) 1/2, and (D) 1/3. Data are presented as plots of ln (c) vs. radius^2, where c represents the absorbance at 562 nm.

Table 4. Measured and Calculated Molecular Weights of the Aggregates Derived from the Observations of Sedimentation-Equilibrium Ultracentrifugation

A/B ratio	M_{found}	M_{calcd}	Formula
A	17942	17942	A_2
A/B =1/1	28070	28763	A_3B_3
A/B =1/2	31606	30612	A_3B_6
A/B =1/3	32952	32463	A_3B_9

A and the **A/B** = 1/1, 1/2, and 1/3 solutions. The ln (c) vs. radius^2 plots of these solutions are shown in Fig. 7. The linearity of these plots indicates the homogeneities of these solutions in molecular weight. The molecular weights derived from this experiment are given in Table 4 along with those calculated for a comparison. The partial specific volume of the peptide moiety was calculated to be 0.736 from the amino acid composition of $PepA_{18}$ using those of individual residues. However, this value was not adopted here, since it did not take into account ZnTAPP and hemin. Instead, analyses were carried out using the value (0.761), which was recalculated to reproduce the theoretical molecular weight of $\mathbf{A}_2$ within the rational range of the partial specific volume for the solution that contains only **A**. On the other hand, the effect of TFE on the partial specific volume of individual amino acid is not yet understood; however, the effect is small according to the literature.[65] Although the contribution of hemin was not taken account into the partial specific volume 0.761, the fact that the molecular weights derived for $\mathbf{A}_3\mathbf{B}_3$, $\mathbf{A}_3\mathbf{B}_6$, and $\mathbf{A}_3\mathbf{B}_9$ were close to the calculated ones indicates the small contribution from hemin, as reported by Choma.[12]

As a consequence, the results suggest that **A** exists as a dimer in solution, and that the aggregation number changes from 2 to 3 when **B** is incorporated into **A** (Fig. 8), thus achieving a 12-porphyrin system. The total aspect in the solution can be described by the following equation:

$$3\mathbf{A}_2 \xrightarrow{18\mathbf{B}} 2\mathbf{A}_3\mathbf{B}_9. \quad (1)$$

Our result that **A** forms a dimer in a TFE-containing buffer solution may recall the behavior of the coproporphyrin peptide by Rabanal et al., who also found the dimerization of porphyrin peptides without hemin.[13] However, the mechanisms of dimerization seem to be different from each other. In their system, the peptide itself tends to form a dimer, that is to say, a four-helix bundle; this tendency is strengthened by a face-to-face interaction between the two coproporphyrins, as exhibited by the large (about 20 nm) blue shift of the Soret band. On the contrary, our compound **A** shows only a slight shift (2 nm) and small broadening of the Soret band; therefore, the motive force of the dimerization of **A** is probably attributed to interactions among the peptide moieties. On the other hand, the dimer-to-trimer transformation observed in our system upon the incorporation of hemin is similar to the result by Choma et al., who reported that a monomer was transformed to a dimer along with the incorporation of hemin.[12]

In summary, 1) we succeeded in combining multiple-histidine peptides with porphyrins, and synthesized three compounds, α_4-$(PepA_{18})_n(AG)_{4-n}$-H_2TAPP (n = 1, 3, and 4), consisting of α_4-atropisomer of tetrakis(*o*-aminophenyl)porphyrin and one, three, and four peptide fragments. 2) We found that the combination of DMF/PyBOP/HOAt(HOBt)/DIEA was effective to the coupling of Boc–Glu(OBzl)–Glu(OBzl)–Ala–Leu–Glu(OBzl)–Lys(ClZ)–His–Glu(OBzl)–Lys(ClZ)–Ala–Leu–Glu(OBzl)–Lys(ClZ)–His–Glu(OBzl)–Lys(ClZ)–OH to $(AG)_4$-H_2TAPP or $(AG)_1$(Boc-$AG)_3$-H_2TAPP at low temperature (starting from −45 °C). 3) The obtained compounds showed about 40% helicity in phosphate buffer solutions (pH = 7.0) in the presence of TFE. 4) α_4-$(PepA_{18})_4$-ZnTAPP incorporated up to three equivalents of Fe(III) protoporphyrin IX chloride. 5) α_4-$(PepA_{18})_4$-ZnTAPP exists as a dimer in the buffer solutions containing TFE; however, it transforms to a trimer when incorporates Fe(III) protoporphyrin IX chloride into it.

Experimental

1. Materials. All of the amino acids derivatives (L form) were purchased from Peptide Institute Inc. PyBOP and TBTU were purchased from Calbiochem-Novabiochem. HOAt and HATU were purchased from Millipore Co. The other reagents and solvents were obtained commercially and were used without further purification, except for the cases noted below. CH_2Cl_2, DIEA, NMM, TEA, and acetonitrile for synthetic use were distilled from CaH_2. DMSO was distilled under reduced pressure from CaH_2. DMF was distilled under reduced pressure from CaH_2 and then from BaO below 60 °C. NMP was dried over molecular sieves and distilled under reduced pressure. Diethyl ether and THF were distilled from $LiAlH_4$. Boc–His(Boc)[35] and Boc-amino acid phenacyl esters[33] (Boc–Lys(ClZ)–OPac and Boc–Glu(OBzl)–OPac) were prepared according to the reported procedures.

In the syntheses of the intermediates, Boc groups were deprotected with TFA or 4 M-HCl/dioxane, and Pac esters were cleaved with Zn powder in 90% AcOH according to the literature.[44] The coupling reactions were carried out by the usual procedure unless otherwise noted. The reaction mixture was concentrated and treated in the following way. When compounds are soluble in chloroform, they were successively washed in the liquid phase with a 10%

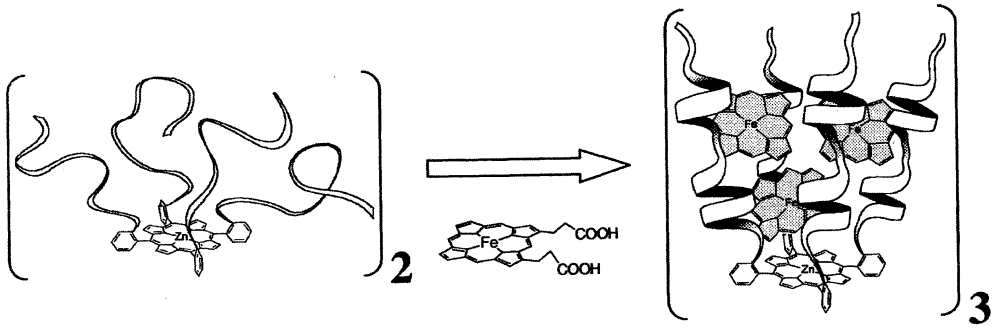

Fig. 8. Dimer–trimer transformation upon addition of hemin chloride.

citric acid aqueous solution, saturated sodium hydrogencarbonate ($NaHCO_3$) aqueous solution, and water. In the other cases, compounds were washed in the solid phase on a fine glass filter. The preparation of H_2TAPP and the separation of the α_4-atropisomer were done according to the literature.[23,55,56] All experiments involving porphyrins were performed in the dark.

2. Analyses. Elemental analyses were performed by Yanaco CHN CORDER MT-5. TLC analyses were carried out on silica-gel 60 F254 (Merck) precoated plates using the following eluents: A, $CHCl_3$–MeOH (90 : 10); B, $CHCl_3$–MeOH (97 : 3). Silica-gel column chromatographies were performed with Wakogel C-200 (Wako). HPLC analysis was carried out on a Shimadzu equipment consisting of two LC-6A pumps, a SCL-6A controller, a SPD-6AV variable-wavelength UV monitor, and a C-R6A data processor chart recorder. The columns used were: Shim-pack CLC-ODS(M) (Shimadzu; 4.6×250 mm) for the analyses of all compounds and the calculation of k' value; Shim-pack PREP-ODS(H) (Shimadzu; 20×250 mm) for the preparative of **9-1**, **9-3**, and **9-4**; Asahipak ODP-50 (Shodex; 4.6×250 mm; 21.5×300 mm) for the analysis and preparative of **6**; CAPCELLPAK C_{18} SG300 (Shiseido, 4.6×250 mm), CAPCELLPAK C_{18} UG120 (Shiseido, 4.6×250 mm), Vydac C_4 (The Separations Group, 4.6×250 mm), COSMOSIL $5C_{18}$-AR (nacalai tesque, 4.6×250 mm), and COSMOSIL $5C_{18}$-AR-300 (nacalai tesque, 4.6×250 mm) for the analyses of **9-3** and **9-4**. HPLC analyses were performed using the following eluents: a, acetonitrile–water (80 : 20); b, acetonitrile–water (72 : 28) containing 0.05% TFA; c, acetonitrile–water (78 : 22) containing 0.05% TFA; d, acetonitrile–water (82 : 18) containing 0.05% TFA; e, MeOH. ^{1}H NMR data were recorded on JEOL JNM-EX270 and JNM-GX500 spectrometers. The spectra were assigned by 2D COSY. Chemical shifts were reported in parts per million (ppm) downfield form. Multiplicities are abbreviated as follows: singlet (s), doublet (d), triplet (t), quartet (q), multiplet (m), and broad (br). FAB mass spectra were obtained with a JEOL JMS-SX102A mass spectrometer using glycerol/3-nitrobenzyl alcohol (1 : 1) as a matrix. ESI mass spectra were obtained with a Finnigan MAT TSQ700 mass spectrometer using 50% aqueous methanol as solvents.

3. UV-vis Spectra. Spectra were measured on a Shimadzu UV-2200A spectrophotometer. The temperature was maintained at 25.0 °C (±0.1 °C) with a Peltier-effect thermomodule equipped with a computer-controlled power MOS FET (homemade). The concentrations of the stock solutions of α_4-$(PepA_{18})_4$-ZnTAPP were determined by comparing the integrated intensities of the peaks of the Soret band in solutions, containing 50 mM Triton X-100 and 20 mM phosphate buffer (pH 7.0), with that of α_4-$(Boc\text{-}AG)_4$-ZnTAPP in methanol, containing 50 mM Triton X-100 and 150 mM imidazole. The practical formula of α_4-$(Boc\text{-}AG)_4$-ZnTAPP was determined by elemental analysis.

4. Circular Dichroism. Circular dichroism spectra were recorded on JASCO J600 and J725 spectropolarimeters using a quartz cell with 0.1 cm optical-path length at 25.0 °C (±0.1°C). The instrument was calibrated with ammonium *d*-camphor-10-sulfonate. The ellipticities are expressed as mean residue ellipticities, unless otherwise noted.

5. Sedimentation Equilibrium Ultracentrifugation. Sedimentation equilibrium ultracentrifugation analyses were performed using a Beckman XL-I analytical ultracentrifuge equipped with an An60Ti rotor. The cell was assembled from double-sector centerpieces and sapphire windows, then loaded with samples (13 μM **A** only, **A/B** = 1/1, 1/2, and 1/3). A buffer containing 15% TFE, 100 mM NaCl, and 20 mM sodium phosphate at pH 7.0 was used. The samples were centrifuged at 25 °C and 28000 rpm for 20 h for equilibration. The distribution of the species equilibrated under centrifugal force within the cell was determined by measuring the absorbance at 363, 410, 530, and 562 nm with an optical scanner. The establishment of equilibrium was judged when successive radial scans were identical. The UV-vis spectra (300—700 nm), which were recorded at four appropriate radial positions, were almost identical to those of the initial samples before centrifugation. The rotor speed was then increased to 50000 rpm to obtain the baseline optical density for analyses. The data at the four wavelength points, which were analyzed using the XL-A/XL-I Data Analysis Software Version 4.0 (Beckman Instruments), yielded the same results. The density of the buffer solution (25 °C) used to determine the molecular weights was 1.072. The partial specific volume was determined from the theoretical molecular weight (see section of Results and Discussion).

6. Synthesis. Boc–Glu(OBzl)–Lys(ClZ)–OPac. Boc–Lys(ClZ)–OPac (24.1 g, 45.2 mmol) was treated with TFA. The salt was dissolved in DMF (40 ml), which was immediately added to the HOBt ester of Boc–Glu(OBzl) preformed from Boc–Glu(OBzl) (17.7 g, 52.7 mmol), HOBt (7.12 g, 52.7 mmol), and EDC·HCl (10.1 g, 52.7 mmol) in CH_2Cl_2–DMF (40 ml, 1 : 1) at 0 °C. DIEA (23.0 ml, 132 mmol) was then slowly added to this solution and the mixture was stirred for 16 h. The product was recrystallized from CH_2Cl_2–diethyl ether. Yield 28.7 g (38.2 mmol, 84.5%); TLC R_f(A) 0.82; HPLC k'(a) 1.7; ^{1}H NMR (DMSO) δ = 8.29 (d, J = 11 Hz, 1H, Lys–NH), 7.94 (d, J = 8 Hz, 2H, OPac–ArH), 7.69 (t, J = 11 Hz, 1H, OPac–ArH), 7.55 (t, J = 8 Hz, 2H, OPac–ArH), 7.47 (t, J = 3 Hz, 2H, ClZ–ArH), 7.32 (m, 8H, Lys–ϵNH, OBzl–ArH, ClZ–ArH), 6.95 (d, J = 5.5 Hz, 1H, Glu–NH), 5.19 (dd, J = 16, 32.5 Hz, 2H, OPac–CH_2), 5.09 and 5.06 (2s, 4H, OBzl–CH_2, ClZ–CH_2), 4.37 and 4.03 (2m, 2H, Lys–αCH, Glu–αCH), 3.02 (m, 2H, Lys–ϵCH_2), 2.40 (t, J = 5.5 Hz, 2H, Glu–γCH_2), 2.00—1.61 (m, 4H, Lys–βCH_2, Glu–βCH_2), 1.44 (s br, 4H, Lys–γCH_2, δCH_2), and 1.35 (s, 9H, Boc–CH_3). FAB MS Found: *m/z* 752. Calcd for $C_{39}H_{46}ClN_3O_{10}$+H$^+$: (M+H)$^+$, 752.

Boc–Leu–Glu(OBzl)–Lys(ClZ)–OPac. Boc–Glu(OBzl)–Lys(ClZ)–OPac was deprotected, then coupled to Boc–Leu·H_2O with NMM, HOBt, and EDC·HCl in DMF. The product was recrystallized from CH_2Cl_2–$CHCl_3$–diethyl ether. Yield 18.5 g (21.4 mmol, 99.5%); TLC R_f(A) 0.70; HPLC k'(a) 2.3; ^{1}H NMR (DMSO) δ = 8.40 (d, J = 8 Hz, 1H, Lys–NH), 7.95 (d, J = 8 Hz, 2H, OPac–ArH), 7.84 (d, J = 8 Hz, 1H, Glu–NH), 7.70 and 7.55 (2t, $J = J'$ = 8 Hz, 3H, OPac–ArH), 7.47 (t, J = 5.5 Hz, 2H, ClZ–ArH), 7.33 (m, 8H, Lys–ϵNH, OBzl–ArH, ClZ–ArH), 6.97 (d, J = 8 Hz, 1H, Leu–NH), 5.51 (dd, J = 16, 30 Hz, 2H, OPac–CH_2), 5.09 and 5.04 (2s, 4H, OBzl–CH_2, ClZ–CH_2), 4.37 and 3.95 (2m, 3H, Leu–αCH, Glu–αCH, Lys–αCH), 3.01 (m, 2H, Lys–ϵCH_2), 2.39 (t, J = 8 Hz, 2H, Glu–γCH_2), 2.05—1.50 (m, 5H, Leu–γCH, Glu–βCH_2, Lys–βCH_2), 1.41 (m, 6H, Leu–βCH_2, Lys–γCH_2, δCH_2), 1.35 (s, 9H, Boc–CH_3), and 0.84 (t, J = 5.5 Hz, 6H, Leu–δCH_3). FAB MS: Found: *m/z* 865. Calcd for $C_{45}H_{57}ClN_4O_{11}$+H$^+$: (M+H)$^+$, 865.

Boc–Ala–Leu–Glu(OBzl)–Lys(ClZ)–OPac, 1. Boc–Leu–Glu(OBzl)–Lys(ClZ)–OPac was deprotected, then coupled to Boc–Ala with NMM, HOBt, and EDC·HCl in DMF. The product was recrystallized from CH_2Cl_2–diethyl ether. Yield 19.8 g (21.1 mmol, 99.0%); TLC R_f(B) 0.36; HPLC k'(a) 1.8; ^{1}H NMR (DMSO) δ = 8.35 (d, J = 8 Hz, 1H, Lys–NH), 7.95 (d, J = 8 Hz, 3H, Glu–NH, OPac–ArH), 7.81 (d, J = 8 Hz, 1H, Leu–NH), 7.70 and 7.55 (2t, $J = J'$ = 8 Hz, 3H, OPac–ArH), 7.47 (t, J = 5.5 Hz, 2H, ClZ–ArH), 7.33 (m, 8H, Lys–ϵNH, OBzl–ArH, ClZ–ArH), 6.97 (d, J = 8 Hz, 1H, Ala–NH), 5.51 (dd, J = 16, 31 Hz, 2H, OPac–CH_2), 5.09 and 5.04 (2s, 4H, OBzl–CH_2, ClZ–CH_2), 4.34 (m, 3H, Leu–αCH, Glu–αCH, Lys–αCH), 3.95 (m, 1H, Ala–αCH), 3.02 (m, 2H,

Lys–ϵCH$_2$), 2.38 (t, J = 8 Hz, 2H, Glu–γCH$_2$), 2.05—1.55 (m, 5H, Leu–γCH, Glu–βCH$_2$, Lys–βCH$_2$), 1.44 (s br, 6H, Leu–βCH$_2$, Lys–γCH$_2$, δCH$_2$), 1.35 (s, 9H, Boc–CH$_3$), 1.14 (d, J = 5.5 Hz, 3H, Ala–βCH$_3$), and 0.82 (dd, J = 5.5, 9.5 Hz, 6H, Leu–δCH$_3$). FAB MS Found: m/z 936. Calcd for $C_{48}H_{62}ClN_5O_{12}$+H$^+$: (M+H)$^+$, 936. Found: C, 61.29; H, 6.61; N, 7.68%. Calcd for $C_{48}H_{62}ClN_5O_{12}$: C, 61.56; H, 6.67; N, 7.48%.

Boc–His(Boc)–Glu(OBzl)–Lys(ClZ)–OPac, 2. Boc–Glu(OBzl)–Lys(ClZ)–OPac was deprotected, then coupled to Boc–His(Boc)·DCHA with NMM, HOBt, and EDC·HCl in DMF. The product was recrystallized from MeOH–CH$_2$Cl$_2$–diethyl ether. Yield 16.4 g (16.6 mmol, 82.0%); TLC R_f(A) 0.54; HPLC k'(a) 2.4; ^{1}H NMR (DMSO) δ = 8.52 (d, J = 8 Hz, 1H, Lys–NH), 8.08 (s, 1H, His–ImH), 7.94 (m, 3H, OPac–ArH, Glu–NH), 7.69 and 7.55 (2t, $J = J'$ = 8 Hz, 3H, OPac–ArH), 7.46 (t, J = 5.5 Hz, 2H, ClZ–ArH), 7.33 (m, 8H, Lys–ϵNH, OBzl–ArH, ClZ–ArH), 7.21 (s, 1H, His–ImH), 6.92 (d, J = 8 Hz, 1H, His–NH), 5.52 (dd, J = 16, 31 Hz, 2H, OPac–CH$_2$), 5.09 and 5.05 (2s, 4H, OBzl–CH$_2$, ClZ–CH$_2$), 4.37 (m, 2H, Glu–αCH, Lys–αCH), 4.21 (m, 1H, His–αCH), 3.01 (m, 2H, Lys–ϵCH$_2$), 2.78 (m, 2H, His–βCH$_2$), 2.40 (t, J = 8 Hz, 2H, Glu–γCH$_2$), 2.06—1.63 (m, 4H, Glu–βCH$_2$, Lys–βCH$_2$), 1.55 (s, 9H, His–Boc–CH$_3$), 1.44 (s br, 4H, Lys–γCH$_2$, δCH$_2$), and 1.32 (s, 9H, Boc–CH$_3$). FAB MS Found: m/z 989. Calcd for $C_{50}H_{61}ClN_6O_{13}$+H$^+$: (M+H)$^+$, 989. Found: C, 59.74; H, 6.09; N, 9.14%. Calcd for $C_{50}H_{61}ClN_6O_{13}$·DMF: C, 59.91; H, 6.45; N, 9.23%.

Boc–Ala–Leu–Glu(OBzl)–Lys(ClZ)–OH, 1–OH. Obtained from **1** by the deprotection of its Pac group. Yield 8.60 g (10.5 mmol, 89.7%); TLC R_f(B) 0.16; HPLC k'(a) 2.0; ^{1}H NMR indicated the disappearance of the phenacyl ester by the absence of peaks at 5.51 ppm.

Boc–Ala–Leu–Glu(OBzl)–Lys(ClZ)–His–Glu(OBzl)–Lys(ClZ)–OPac, 3. Obtained by the coupling of the deprotected **2** with **1**-OH in DMF using PyBOP and DIEA. The product was purified by a silica-gel column chromatography with CHCl$_3$–MeOH (100 : 3) as the eluent. Yield 4.50 g (2.83 mmol, 84.7%); TLC R_f(A) 0.55; HPLC k'(b) 2.4; ^{1}H NMR (DMSO) δ = 8.73 (s br, 1H, Lys–NH), 7.99 (m, 4H, His–NH, Glu–NH, Lys–NH), 7.95 (d, J = 8.5 Hz, 2H, OPac–ArH), 7.83 (d, J = 8.5 Hz, 1H, Leu–NH), 7.69 (t, J = 8 Hz, 1H, OPac–ArH), 7.63 (s, 1H, His–ImH), 7.55 (t, J = 8 Hz, 2H, OPac–ArH), 7.46 (m, 4H, ClZ–ArH), 7.33 (m, 16H, Lys–ϵNH, OBzl–ArH, ClZ–ArH), 6.95 (d, J = 7.5 Hz, 1H, Ala–NH), 6.84 (s, 1H, His–ImH), 5.51 (dd, J = 17, 50 Hz, 2H, OPac–CH$_2$), 5.08 and 5.05 (2d, J = 5.5 Hz, J' = 10 Hz, 8H, OBzl–CH$_2$, ClZ–CH$_2$), 4.48 (m, 1H, His–αCH), 4.41—4.24 and 4.18 (2m, 5H, Leu–αCH, Glu–αCH, Lys–αCH), 3.95 (m, 1H, Ala–αCH), 3.05—2.85 (m, 6H, His–βCH$_2$, Lys–ϵCH$_2$), 2.37 (m, 4H, Glu–γCH$_2$), 2.06—1.17 (m, 19H, Leu–βCH$_2$, γCH, Glu–βCH$_2$, Lys–βCH$_2$, γCH$_2$, δCH$_2$), 1.35 (s, 9H, Boc–CH$_3$), 1.14 (d, J = 7 Hz, 3H, Ala–βCH$_3$), and 0.829 (dd, J = 6.5, 18 Hz, 6H, Leu–δCH$_3$). FAB MS Found: m/z 1590. Calcd for $C_{80}H_{99}Cl_2N_{11}O_{19}$+H$^+$: (M+H)$^+$, 1590. Found: C, 58.97; H, 6.26; N, 9.66%. Calcd for $C_{80}H_{99}Cl_2N_{11}O_{19}$·2H$_2$O: C, 59.10; H, 6.39; N, 9.48%.

Boc–Glu(OBzl)–Glu(OBzl)–OPac, 4. Obtained by the coupling of Boc–Glu(OBzl) and Glu(OBzl)–OPac in DMF by using TBTU and DIEA. The product was purified by a silica-gel column chromatography with CHCl$_3$–MeOH (100 : 1) as the eluent. Yield 6.80 g (10.1 mmol, 67.3%); TLC R_f(A) 0.43; HPLC k'(a) 1.7; ^{1}H NMR (DMSO) δ = 8.39 (d, J = 8 Hz, 1H, Glu–NH), 7.96 (d, J = 8 Hz, 2H, OPac–ArH), 7.70 and 7.56 (2t, $J = J'$ = 8 Hz, 3H, OPac–ArH), 7.33 (m, 10H, OBzl–ArH), 7.00 (d, J = 8 Hz, 1H, Glu–NH), 5.53 (dd, J = 16, 38 Hz, 2H, OPac–CH$_2$), 5.12 and 5.06 (2s, 4H, OBzl–CH$_2$), 4.50 and 3.99 (2m, 2H, Glu–αCH), 2.60 and 2.40 (2t, $J = J'$ = 8 Hz, 4H, Glu–γCH$_2$), 2.29—1.68 (m, 4H, Glu–βCH$_2$), and 1.34 (s, 9H, Boc). FAB MS Found: m/z 675. Calcd for $C_{37}H_{42}N_2O_{10}$+H$^+$: (M+H)$^+$, 675.

Boc–Glu(OBzl)–Glu(OBzl)–OH, 4–OH. Obtained from **4**. Yield 3.28 g (5.89 mmol, 93.4%); TLC R_f(A) 0.11; ^{1}H NMR indicated the disappearance of Pac group (peak at 5.53 ppm).

Boc–Glu(OBzl)–Glu(OBzl)–Ala–Leu–Glu(OBzl)–Lys(ClZ)–His–Glu(OBzl)–Lys(ClZ)–OPac, 5. The heptapeptide **3** was deprotected, then coupled to **4**-OH in DMF using PyBOP and DIEA. The product was reprecipitated from DMF–water. Yield 1.85 g (0.912 mmol, 98.4%); TLC R_f(A) 0.50; HPLC k'(c) 3.0; FAB MS Found: m/z 2028. Calcd for $C_{104}H_{125}Cl_2N_{13}O_{25}$+H$^+$: (M+H)$^+$, 2028. Found: C, 58.77; H, 5.88; N, 8.94%. Calcd for $C_{104}H_{125}Cl_2N_{13}O_{25}$·CF$_3$COOH·H$_2$O: C, 58.94; H, 5.97; N, 8.43%.

Boc–Glu(OBzl)–Glu(OBzl)–Ala–Leu–Glu(OBzl)–Lys(ClZ)–His–Glu(OBzl)–Lys(ClZ)–OH, 5-OH. Obtained from **5** by the cleavage of the Pac group. Yield 0.887 g (0.464 mmol, 94.2%); TLC R_f(A) 0.29; HPLC k'(c) 1.6; ^{1}H NMR indicated the disappearance of Pac group (at 5.52 ppm).

Boc–Glu(OBzl)–Glu(OBzl)–Ala–Leu–Glu(OBzl)–Lys(ClZ)–His–Glu(OBzl)–Lys(ClZ)–Ala–Leu–Glu(OBzl)–Lys(ClZ)–His–Glu(OBzl)–Lys(ClZ)–OPac, 6. The heptapeptide **3** was deprotected with TFA. The TFA salt (639 mg, 0.372 mmol) and the nonapeptide **5**-OH (730 mg, 0.372 mmol) were dissolved in DMF (13 ml), to which HOBt (60.3 mg, 0.446 mmol), PyBOP (232 mg, 0.446 mmol), and DIEA (0.20 ml, 1.1 mmol) were added. The mixture was stirred for 20 h, which was set at −40 °C at the starting point, then gradually raised up to 15 °C. The solution was concentrated and the residue was taken up in chloroform. It was washed with saturated NaHCO$_3$ solution and brine. The product was purified by a preparative RP-HPLC (Asahipak ODP-50, eluent: acetonitrile–water 9 : 1 containing 0.031% TEA). Yield 930 mg (0.275 mmol, 73.9%); TLC R_f(A) 0.47; HPLC k'(d) 4.9; ^{1}H NMR (DMSO) δ = 8.81 and 8.57 (2s br, 2H), 8.22—6.74 (m, 72H), 7.69 and 7.55 (2t, $J = J'$ = 8 Hz, 3H, OPac–ArH), 5.50 (dd, J = 17, 50 Hz, 2H, OPac–CH$_2$), 5.05 (m, 20H, OBzl–CH$_2$, ClZ–CH$_2$), 4.48—3.90 (m, 16H, αCH), 3.03—2.83 (m, 12H, His–βCH$_2$, Lys–ϵCH$_2$), 2.45—2.28 (m, 12H, Glu–γCH$_2$), 2.05—1.10 (m, 57H), and 0.79 (dd, J = 6, 25 Hz, 12H, Leu–δCH$_3$). FAB MS Found: m/z 3381. Calcd for $C_{171}H_{208}Cl_4N_{24}O_{40}$+H$^+$: (M+H)$^+$, 3381.

Boc–Glu(OBzl)–Glu(OBzl)–Ala–Leu–Glu(OBzl)–Lys(ClZ)–His–Glu(OBzl)–Lys(ClZ)–Ala–Leu–Glu(OBzl)–Lys(ClZ)–His–Glu(OBzl)–Lys(ClZ)–OH, 6-OH. Obtained from **6** by the cleavage of Pac group. Yield 358 mg (0.110 mmol, 93.2%); TLC R_f(A) 0.22; HPLC k'(d) 2.7; ^{1}H NMR indicated the disappearance of the Pac group (5.50 ppm). FAB MS Found: m/z 3263. Calcd for $C_{163}H_{202}Cl_4N_{24}O_{39}$+H$^+$: (M+H)$^+$, 3263.

***α*$_4$–(Boc–Gly)$_4$-H$_2$TAPP, 10.** α_4-H$_2$TAPP (300 mg, 0.445 mmol) was dissolved in CH$_2$Cl$_2$ (15 ml) to which NMM (0.39 ml, 3.6 mmol), Boc–Gly (624 mg, 3.56 mmol), and EDC·HCl (819 mg, 4.27 mmol) were added. After stirring for 2 h at −5 °C, then for 2 d at room temperature, the reaction mixture was diluted with 100 ml of chloroform. This solution was washed with 10% citric acid solution (3×100 ml), water (100 ml), saturated NaHCO$_3$ solution (3×100 ml), and water (100 ml), then dried in vacuo. The product was obtained in quantitative yield. This crude product was used for the next synthesis without further purification. The material purified on a silica-gel column (eluent: CHCl$_3$–MeOH 100 : 2) was subjected to ^{1}H NMR, FAB MS, and elemental analysis.[66] TLC R_f(A) 0.66; HPLC k'(e) 1.9.

***α*$_4$–(Boc–Ala–Gly)$_4$-H$_2$TAPP, 11.** Compound **10** (100 mg,

77.0 μmol) was treated with CH_2Cl_2–thioanisole–TFA (1 ml; 3 : 4 : 3 (v/v/v)). The TFA salt (90.5 mg, 66.6 μmol) was dissolved in DMF (4 ml), to which DIEA (47 μl, 270 μmol), Boc–Ala (101 mg, 534 μmol), HOBt (86.5 mg, 640 μmol), and EDC·HCl (123 mg, 640 μmol) were added. After stirring for 2 h at −5 °C and overnight at room temperature, the solution was treated by the same procedure as described in the section of **10**. The product was purified on a silica-gel column with $CHCl_3$–MeOH (97 : 3) as the eluent. Yield 82.6 mg (52.1 μmol, 78.2%); TLC R_f(A) 0.58; HPLC k'(e) 2.0; ^{1}H NMR (DMSO) δ = 8.88 (s, 4H, ArNH), 8.66 (s, 8H, pyrrole–βCH), 8.11 and 7.96 (2d, $J = J'$ = 8 Hz, 8H, ArH), 7.84 (t, J = 8 Hz, 4H, ArH), 7.64 (m, 4H, Gly–NH), 7.59 (t, J = 8 Hz, 4H, ArH), 7.62 (d, J = 5 Hz, 4H, Ala–NH), 3.56 (m, 4H, Ala–αCH), 2.94 (s, 8H, Gly–αCH_2), 1.26 (s, 36H, Boc), 0.61 (d, J = 8 Hz, 12H, Ala–βCH_3), and −2.76 (s, 2H, pyrrole–NH); FAB MS Found: *m/z* 1588. Calcd for $C_{84}H_{98}N_{16}O_{16}$+H$^+$: (M+H)$^+$, 1588. Found: C, 57.56; H, 6.08; N, 12.56%. Calcd for $C_{84}H_{98}N_{16}O_{16}\cdot CHCl_3\cdot 3H_2O$: C, 57.96; H, 6.01; N, 12.73%.

α_4-(Ala–Gly)$_4$–H$_2$TAPP, 7. Obtained from **11** (45 mg, 28.0 μmol) by deprotecting the Boc group with CH_2Cl_2-thioanisole–TFA (0.7 ml; 3 : 4 : 3 (v/v/v)); TLC R_f(A) 0; ^{1}H NMR (DMSO) δ = 9.15 (s, 4H, ArNH), 8.69 (s, 8H, pyrrole–βCH), 8.31 (s br, 4H, Gly–NH), 8.24 (d, J = 8 Hz, 4H, ArH), 7.89 and 7.84 (2d, $J = J'$ = 8 Hz, 8H, ArH), 7.65 (s br, 8H, Ala–NH_2), 7.56 (t, J = 7 Hz, 4H, ArH), 3.54 (s br, 4H, Ala–αCH), 3.15 (s br, 8H, Gly–αCH_2), 1.09 (m, 12H, Ala–βCH_3), and −2.79 (s, 2H, pyrrole–NH).

α_4-(Ala–Gly)$_1$(Boc–Ala–Gly)$_3$-H$_2$TAPP, 8. To a cold (−20 °C) solution of compound **11** (245 mg, 154 μmol) in CH_2Cl_2 (18 ml), thioanisole (0.9 ml, 7.7 mmol) and TFA (0.6 ml, 7.7 mmol) were added. The mixture was stirred for 7 h, which was set at −20 °C at the starting point, then gradually raised up to 0 °C (the reaction was monitored on TLC). The solution was neutralized with TEA, and concentrated. The residue was purified by a preparative silica-gel TLC (developing solvent: $CHCl_3$–MeOH (9 : 1)), which afforded two major bands. The first band was the starting compound **11**, (134 mg, 54.8%). The second band was the target compound. Yield 94.7 mg (59.2 μmol, 38.4%); TLC R_f(A) 0.49; ^{1}H NMR (DMSO) δ = 8.88 (s, 4H, ArNH), 8.69, 8.67 and 8.59 (3s, 8H, pyrrole–βCH), 8.29—7.50 (m, 14H, ArH, Gly–NH, Ala–NH_2), 7.99 (t, J = 8 Hz, 4H, ArH), 7.85 (t, J = 8 Hz, 4H, ArH), 6.66 (m br, 3H, Ala–NH), 3.58 (s br, 4H, Ala–αCH), 3.04 and 2.94 (2s br, 8H, Gly–αCH_2), 1.27 (s, 27H, Boc), 0.70 (m, 9H, Ala–βCH_3), 0.27 (s br, 3H, Ala–βCH_3), and −2.77 (s br, 2H, pyrrole–NH); FAB MS Found: *m/z* 1487. Calcd for $C_{79}H_{90}N_{16}O_{14}$+H$^+$: (M+H)$^+$, 1487. Found: C, 59.40; H, 5.79; N, 13.67% Calcd for $C_{79}H_{90}N_{16}O_{14}\cdot CHCl_3\cdot H_2O$: C, 59.13; H, 5.77; N, 13.79%.

α_4-(Glu–Glu–Ala–Leu–Glu–Lys–His–Glu–Lys–Ala–Leu–Glu–Lys–His–Glu–Lys–Ala–Gly)$_4$-H$_2$TAPP, α_4-(PepA$_{18}$)$_4$-H$_2$ TAPP, 9-4. To a cold (−45 °C) solution of the peptide fragment **6**-OH (59.2 mg, 17.5 μmol) and the porphyrin fragment **7** (4.8 mg, 2.92 μmol) in DMF (1 ml), HOAt (3.6 mg, 26.3 μmol), PyBOP (12.6 mg, 24.2 μmol), and DIEA (8.1 μl, 46.7 μmol) were added. After 31 h stirring, which was set at −45 °C at the starting point and then gradually raised up to room temperature, the solution was concentrated. The residue was treated with CH_2Cl_2–thioanisole–TFA (7 ml; 2 : 3 : 2 (v/v/v)) for 1 h at 0 °C and for 20 min at room temperature to deprotect Boc groups; the solvents were then removed in vacuo. The residue was dissolved in TFA (3.9 ml), to which thioanisole (620 μl, 5.3 mmol), *m*-cresol (25 μl, 0.23 mmol), and TMSOTf (1.0 ml, 5.3 mmol) were added at −5 °C. The solution was stirred for 1.5 h at 0 °C, and diethyl ether was added. The resulting green powder was collected by centrifugation and washed with diethyl ether. The deprotected compound was dissolved in a small amount of water and the solution was adjusted to pH 8 with TEA. After the addition of 1 M NH_4F (485 μl), the solution was stirred for 30 min at 0 °C. Next, it was desalted on a Sep-Pak tC$_{18}$ (Waters, eluent: 0.05% aqueous TFA and 32% aqueous acetonitrile containing 0.05% TFA). Purification was carried out by a preparative RP-HPLC (Shim-pack PREP-ODS(H), eluent: water–acetonitrile (0.05% TFA) with acetonitrile gradient from 10 to 40%). The eluate corresponding to the main peak was collected and lyophilized. Yield 11 mg (1.2 μmol, 42%); ESI MS Found: *m/z* 8909.3. Calcd for $C_{400}H_{610}N_{112}O_{120}$: M, 8902.5 (monoisotopic), 8907.9 (average).

α_4-(Glu–Glu–Ala–Leu–Glu–Lys–His–Glu–Lys–Ala–Leu–Glu–Lys–His–Glu–Lys–Ala–Gly)$_3$(Ala–Gly)$_1$-H$_2$TAPP, α_4-(PepA$_{18}$)$_3$(Ala–Gly)$_1$-H$_2$TAPP, 9-3. To a cold (−45 °C) solution of the peptide fragment **6**-OH (18.5 mg, 5.5 μmol) and the porphyrin fragment **7** (2.3 mg, 1.4 μmol) in DMF (0.8 ml), HOBt (0.80 mg, 5.9 μmol), PyBOP (3.1 mg, 5.9 μmol), and DIEA (2.9 μl, 16.4 μmol) were added. After 6 h stirring, which was set at −45 °C at the starting point and then gradually raised up to −10 °C, the solution was concentrated. The deprotection was carried out as described in the section of **9-4** with CH_2Cl_2–thioanisole–TFA (1.4 ml; 2 : 3 : 2 (v/v/v)), then with TFA (1.7 ml), thioanisole (290 μl, 2.5 mmol), *m*-cresol (12 μl, 110 μmol), and TMSOTf (480 μl, 2.5 mmol). Purification was carried out by a preparative RP-HPLC (eluent: water–acetonitrile (0.05% TFA) with acetonitrile gradient from 10 to 40%). Yield 2.8 mg (0.40 μmol, 29%); ESI MS Found: *m/z* 6978.0. Calcd for $C_{316}H_{474}N_{88}O_{92}$: M, 6973.5 (monoisotopic), 6977.8 (average). **9-4** was also formed and purified, yield 1.3 mg (0.15 μmol, 11%).

α_4-(Glu–Glu–Ala–Leu–Glu–Lys–His-Glu–Lys–Ala–Leu–Glu–Lys–His–Glu–Lys–Ala–Gly)$_1$(Ala–Gly)$_3$-H$_2$TAPP, α_4-(PepA$_{18}$)$_1$(Ala–Gly)$_3$-H$_2$TAPP, 9-1. To a cold (−50 °C) solution of the peptide fragment **6**-OH (2.0 mg, 0.59 μmol) and the porphyrin fragment **8** (0.95 mg, 0.59 μmol) in DMF (0.1 ml), HOBt (0.096 mg, 0.71 μmol), PyBOP (0.37 mg, 0.71 μmol), and DIEA (0.31 μl, 1.8 μmol) were added. After 5 h stirring, which was set at −50 °C at the starting point and then gradually raised up to −25 °C, the solution was concentrated. The deprotection was carried out as described in the section of **9-4** with CH_2Cl_2–thioanisole–TFA (0.7 ml; 2 : 3 : 2 (v/v/v)), then with TFA (0.7 ml), thioanisole (45 μl, 380 μmol), *m*-cresol (1.8 μl, 17 μmol), and TMSOTf (73 μl, 380 μmol). Purification was carried out by a preparative RP-HPLC (eluent: water–acetonitrile (0.05% TFA) with acetonitrile gradient from 10 to 90%). Yield 1.8 mg (0.58 μmol, 98%); ESI MS Found: *m/z* 3117.7. Calcd for $C_{148}H_{202}N_{40}O_{36}$: M, 3115.5 (monoisotopic), 3117.5 (average).

α_4-(Glu–Glu–Ala–Leu–Glu–Lys–His–Glu–Lys–Ala–Leu–Glu–Lys–His–Glu–Lys–Ala–Gly)$_4$-ZnTAPP, α_4-(PepA$_{18}$)$_4$-Zn TAPP, A. The solution of **9-4** (1.8 mg, 0.2 μmol) and $ZnCl_2$ (0.27 mg, 2.0 μmol) in 12 mM ammonium acetate buffer pH 7.0 (0.8 ml) was gently stirred at r.t. for 3 h. The metalation was monitored on RP-HPLC and UV-vis spectrophotometer. Then, 100 mM EDTA·2Na (0.5 ml) was added. The solution was applied to Sephadex G25 (eluent: 10 mM ammonium acetate pH 7.0). The eluate corresponding to the main peak was collected and lyophilized. Yield 1.7 mg (0.19 μmol, 95%); ESI MS Found: *m/z* 8971.0. Calcd for $C_{400}H_{608}N_{112}O_{120}Zn$: M, 8964.4 (monoisotopic), 8971.3 (average).

We thank Dr. Yutaka Ohtsu and Dr. Takashi Ogawa of

Shiseido Corp. and Nacalai Tesque, Inc. for HPLC columns. This work was partly supported by Grants-in-Aid for Scientific Research Nos. 07640763 and 08454213 from the Ministry of Education, Science, Sports and Culture.

References

1) H. Mihara, Y. Haruta, S. Sakamoto, N. Nishino, and H. Aoyagi, *Chem. Lett.*, **1996**, 1.

2) H. Mihara, K. Tomizaki, T. Fujimoto, S. Sakamoto, H. Aoyagi, and N. Nishino, *Chem. Lett.*, **1996**, 187.

3) D. R. Benson, B. R. Hart, X. Zhu, and M. B. Doughty, *J. Am. Chem. Soc.*, **117**, 8502 (1995).

4) C. T. Choma, K. Kaestle, K. S. Åkerfeldt, R. M. Kim, J. T. Groves, and W. F. DeGrado, *Tetrahedron Lett.*, **35**, 6191 (1994).

5) K. S. Åkerfeldt, R. M. Kim, D. Camac, J. T. Groves, J. D. Lear, and W. F. DeGrado, *J. Am. Chem. Soc.*, **114**, 9656 (1992).

6) T. Arai, K. Kobata, H. Mihara, T. Fujimoto, and N. Nishino, *Bull. Chem. Soc. Jpn.*, **68**, 1989 (1995); H. Mihara, N. Nishino, R. Hasegawa, and T. Fujimoto, *Chem. Lett.*, **1992**, 1805.

7) T. Sasaki and E. T. Kaiser, *J. Am. Chem. Soc.*, **111**, 380 (1989).

8) H. K. Rau and W. Haehnel, *J. Am. Chem. Soc.*, **120**, 468 (1998).

9) P. A. Arnold, W. R. Shelton, and D. R. Benson, *J. Am. Chem. Soc.*, **119**, 3181 (1997).

10) S. Sakamoto, S. Sakurai, A. Ueno, and H. Mihara, *Chem. Commun.*, **1997**, 1221.

11) D. E. Robertson, R. S. Farid, C. C. Moser, J. L. Urbauer, S. E. Mulholland, R. Pidikiti, J. D. Lear, A. J. Wand, W. F. DeGrado, and P. L. Dutton, *Nature*, **368**, 425 (1994).

12) C. T. Choma, J. D. Lear, M. J. Nelson, P. L. Dutton, D. E. Robertson, and W. F. DeGrado, *J. Am. Chem. Soc.*, **116**, 856 (1994).

13) F. Rabanal, W. F. DeGrado, and P. L. Dutton, *J. Am. Chem. Soc.*, **118**, 473 (1996).

14) T. B. Karpishin, T. A. Vannelli, and K. J. Glover, *J. Am. Chem. Soc.*, **119**, 9063 (1997).

15) J. Morais, P. N. Palma, C. Frazão, J. Caldeira, J. LeGall, I. Moura, J. J. G. Moura, and M. A. Carrondo, *Biochemistry*, **34**, 12830 (1995).

16) N. Igarashi, H. Moriyama, T. Fujiwara, Y. Fukumori, and N. Tanaka, *Nature Struct. Biol.*, **4**, 276 (1997).

17) G. McDermott, S. M. Prince, A. A. Freer, A. M. Hawthornthwaite-Lawless, M. Z. Papiz, R. J. Cogdell, and N. W. Isaacs, *Nature*, **374**, 517 (1995).

18) B. W. Matthews, R. E. Fenna, M. C. Bolognesi, M. F. Schmid, and J. M. Olson, *J. Mol. Biol.*, **131**, 259 (1979).

19) J. Deisenhofer, O. Epp, K. Miki, R. Huber, and H. Michel, *Nature*, **318**, 618 (1985).

20) M. Ushiyama, Y. Katayama, and T. Yamamura, *Chem. Lett.*, **1995**, 395.

21) J. P. Collman, J. I. Brauman, K. M. Doxsee, T. R. Halbert, E. Bunnenberg, R. E. Linder, G. N. LaMar, J. D. Gaudio, G. Lang, and K. Spartalian, *J. Am. Chem. Soc.*, **102**, 4182 (1980).

22) M. Ushiyama, F. Arisaka, and T. Yamamura, *Chem. Lett.*, **1999**, 127.

23) J. P. Collman, R. R. Gagne, C. A. Reed, T. R. Halbert, G. Lang, and W. T. Robinson, *J. Am. Chem. Soc.*, **97**, 1427 (1975).

24) M. Mutter and S. Vuilleumier, *Angew. Chem., Int. Ed. Engl.*, **28**, 535 (1989).

25) P. Prevelige, Jr., and G. D. Fasman, "Prediction of Protein Structure and the Principles of Protein Conformation," ed by G. D. Fasman, Plenum Press, New York (1989), pp. 391—416.

26) F. M. Richards, *Ann. Rev. Biophys. Bioeng.*, **6**, 151 (1977).

27) The areas of solvent-accessible surfaces were calculated for the non-bundle and helix-bundle states by using ms program, which is included in MidasPlus (note 29). The decrease of the area accompanying with helix-bundle formation was computed to ca. 1000 $Å^2$, from which the stabilization free energy on the ice-shell liquidation was derived according to Ref. 26.

28) The detail will be reported elsewhere.

29) Molecular graphics images were produced using the MidasPlus software system from the Computer Graphics Laboratory, University of California, San Francisco: T. E. Ferrin, C. C. Huang, L. E. Jarvis, and R. Langridge, *J. Mol. Graphics*, **6**, 13 (1988).

30) S. J. Weiner, P. A. Kollman, D. T. Nguyen, and D. A. Case, *J. Comput. Chem.*, **27**, 230 (1986).

31) Due to its impossibility of purification of intermediates, the solid-phase peptide synthesis is inferior to the liquid phase method to make sure the preparation of high purity product (Ref. 24). Furthermore, the purification of protected peptide is generally difficult because of its low solubility (Ref. 32), even if the peptide is carefully cleaved from the resin without deprotection of the side chains.

32) H. Hojo and S. Aimoto, *Bull. Chem. Soc. Jpn.*, **64**, 111 (1991).

33) G. C. Stelakatos, A. Paganou, and L. Zervas, *J. Chem. Soc. C*, **1966**, 1191.

34) Hereafter, we use abbreviations ***n***-OH and H_2N-***n***, for the phenacyl and Boc cleaved forms, respectively, where ***n*** means the substance number **1** to **6**. For example, **6**-OH equals Boc–Glu(OBzl)–Glu(OBzl)–Ala–Leu–Glu(OBzl)–Lys(ClZ)–His–Glu(OBzl)–Lys(ClZ)–Ala–Leu–Glu(OBzl)–Lys(ClZ)–His–Glu(OBzl)–Lys(ClZ)–OH.

35) D. L. Nguyen, R. Seyer, A. Heitz, and B. Castro, *J. Chem. Soc., Perkin Trans. 1*, **1985**, 1025.

36) In our attempt to hydrolyze the α_4-Gly-phenacyl ester of α_4-tetrakis(*o*-carboxyphenyl)porphyrin, α_4-H_2TCPP-(Gly–OPac)$_4$, the application of Zn powder caused a fast remarkable bleaching of this compound.

37) N. Fujii, A. Otaka, O. Ikemura, M. Hatano, A. Okamachi, S. Funakoshi, M. Sakurai, T. Shioiri, and H. Yajima, *Chem. Pharm. Bull.*, **35**, 3447 (1987).

38) N. Fujii, A. Otaka, O. Ikemura, K. Akaji, S. Funakoshi, Y. Hayashi, Y. Kuroda, and H. Yajima, *J. Chem. Soc., Chem. Commun.*, **1987**, 274.

39) T. Fujii, T. Kimura, and S. Sakakibara, *Bull. Chem. Soc. Jpn.*, **49**, 1595 (1976).

40) N. Fujii, M. Sakurai, K. Akaji, M. Nomizu, H. Yajima, K. Mizuta, M. Aono, M. Moriga, K. Inoue, R. Hosotani, and T. Tobe, *Chem. Pharm. Bull.*, **34**, 2397 (1986).

41) R. Seyer, A. Aumelas, A. Caraty, P. Rivaille, and B. Castro, *Int. J. Peptide Protein Res.*, **35**, 465 (1990).

42) T. Kimura, M. Takai, Y. Masui, T. Morikawa, and S. Sakakibara, *Biopolymers*, **20**, 1823 (1981).

43) P. Rivaille, J. P. Gautron, B. Castro, and G. Milhaud, *Tetrahedron*, **36**, 3413 (1980).

44) C-B. Xue, A. Ewenson, J. M. Becker, and F. Naider, *Int. J. Peptide Protein Res.*, **36**, 362 (1990).

45) The phenacyl esters of **1**, **4**, **5**, and **6** were efficiently removed by Zn/90% acetic acid.

46) a) This side reaction gave only one by-product which showed the same mass number as **6**, which shows the possibility of the

racemization of **6** at the coupling. b) Histidine easily racemizes via the steric interaction of the imidazole group and the carboxyl group, or the elimination of the α-hydrogen by the imidazole group (Refs. 47 and 48). The molecular modeling of peptide fragments **3**-OH and **5**-OH showed that the imidazole groups of their histidines, which are placed on the third residues from the carboxyl termini, can take close positions to their C-terminal amino acids, which might cause the similar racemization effect on the C-terminal residues.

47) M. Bodanszky, "Peptide Chemistry: A Practical Textbook," 2nd rev. ed, Springer-Verlag, Berlin (1993), pp. 117—128.

48) G. Barany and R. B. Merrifield, "The Peptides: Analysis, Synthesis, Biology," ed by E. Gross and J. Meienhofer, Academic Press, New York (1979), Vol. 2, pp. 179—189.

49) L. A. Carpino, *J. Am. Chem. Soc.*, **115**, 4397 (1993).

50) L. A. Carpino, A. EI-Faham, C. A. Minor, and F. Albericio, *J. Chem. Soc., Chem. Commun.*, **1994**, 201.

51) 80% yield was achieved at this point.

52) B. Castro, J.-R. Dormoy, B. Dourtoglou, G. Evin, and C. Selve, J-C. Ziegler, *Synthesis*, **1976**, 751.

53) J. Coste, D. Le-Nguyen, and B. Castro, *Tetrahedron Lett.*, **31**, 205 (1990).

54) The aqueous acetonitrile solution containing TFA or AcOH achieved good separation, but the TEA-containing eluent also achieved a good result with less amount of water. This was advantageous to treat the compound, because the mixing of water decreased the solubility of compound.

55) T. N. Sorrell, *Inorg. Synth.*, **20**, 161 (1980).

56) J. Lindsey, *J. Org. Chem.*, **45**, 5215 (1980).

57) R. A. Freitag, J. A. Mercer-Smith, and D. G. Whitten, *J. Am. Chem. Soc.*, **103**, 1226 (1981).

58) In the presence of **6**-OH, such instability of the porphyrin fragment was not observed.

59) Y. Ohtsu, Y. Shiojima, T. Okumura, J. Koyama, K. Nakamura, O. Nakata, K. Kimata, and N. Tanaka, *J. Chromatogr.*, **481**, 147 (1989).

60) J. Koyama, J. Nomura, Y. Ohtsu, O. Nakata, and M. Takahashi, *Chem. Lett.*, **1990**, 687.

61) A. Cammers-Goodwin, T. J. Allen, S. L. Oslick, K. F. McClure, J. H. Lee, and D. S. Kemp, *J. Am. Chem. Soc.*, **118**, 3082 (1996).

62) The helicity was derived from $[\theta]^{obs}/[\theta]^{max}$, where $[\theta]^{max} = ((n-4)/n)[\theta]^{\infty}$ = the maximal mean residue ellipticity value for chain length, n = the number of residues, and $[\theta]^{\infty} = -40000$ deg cm^2 dmol^{-1} (Ref. 63).

63) P. C. Lyu, J. C. Sherman, A. Chen, and N. R. Kallenbach, *Proc. Natl. Acad. Sci. U.S.A.*, **88**, 5317 (1991).

64) I. Hamachi, K. Nakamura, A. Fujita, and T. Kunitake, *J. Am. Chem. Soc.*, **115**, 4966 (1993).

65) C. E. MacPhee, M. A. Perugini, W. H. Sawyer, and G. J. Howlett, *FEBS Lett.*, **416**, 265 (1997).

66) ^{1}H NMR, FAB MS, and elemental analysis were reported in the Ref. 20.